Ten-year monitoring of high-rise building columns using long-gauge fiber optic sensors

2013 Smart Mater. Struct. 22 055030

(http://iopscience.iop.org/0964-1726/22/5/055030)

Smart Mater. Struct. **22** (2013) 055030 (15pp) doi:10.1088/0964-1726/22/5/055030

Ten-year monitoring of high-rise building columns using long-gauge fiber optic sensors

B Glisic[1], D Inaudi[2], J M Lau[3] and C C Fong[3]

[1] Princeton University E330 EQuad, Princeton, NJ 08544, USA
[2] SMARTEC SA, Via Pobiette 11, 6928 Manno, Switzerland
[3] Housing and Development Board (HDB), HDB Hub, 480 Lorong 6 Toa Payoh, 310480, Singapore

E-mail: bglisic@princeton.edu

Received 24 January 2013, in final form 28 January 2013
Published 18 April 2013
Online at stacks.iop.org/SMS/22/055030

Abstract
A large-scale lifetime building monitoring program was implemented in Singapore in 2001. The monitoring aims of this unique program were to increase safety, verify performance, control quality, increase knowledge, optimize maintenance costs, and evaluate the condition of the structures after a hazardous event. The first instrumented building, which has now been monitored for more than ten years, is presented in this paper. The long-gauge fiber optic strain sensors were embedded in fresh concrete of ground-level columns, thus the monitoring started at the birth of both the construction material and the structure. Measurement sessions were performed during construction, upon completion of each new story and the roof, and after the construction, i.e., in-service. Based on results it was possible to follow and evaluate long-term behavior of the building through every stage of its life. The results of monitoring were analyzed at a local (column) and global (building) level. Over-dimensioning of one column was identified. Differential settlement of foundations was detected, localized, and its magnitude estimated. Post-tremor analysis was performed. Real long-term behavior of concrete columns was assessed. Finally, the long-term performance of the monitoring system was evaluated. The researched monitoring method, monitoring system, rich results gathered over approximately ten years, data analysis algorithms, and the conclusions on the structural behavior and health condition of the building based on monitoring are presented in this paper.

1. Introduction

In the case of residential, high-rise buildings, malfunctioning can have serious consequences. The most severe is an accident involving human victims. Even when there is no loss of life, inhabitants suffer significantly if their building is partially or completely out of service. Residential buildings that undergo an extreme event, such as earthquake, explosion, or terrorist acts, are usually evacuated and there is an immediate need to estimate their structural condition in order to mitigate the crisis (e.g. [1]).

Structural health monitoring is becoming recognized in the domain of civil engineering as the proper means to increase safety and optimize the operational and maintenance costs of the structures. Detection of unusual behavior (e.g. due to damage or deterioration) can be used to assess deviations from the design performance. Monitoring data can be integrated in structural management systems and increase the quality of decisions by providing reliable and unbiased information.

In spite of its great potential, SHM is not applied in a widespread or systematic manner to residential buildings. Among others, an important reason for this is the lack of generic monitoring solutions that are reliable and affordable, which is in part a consequence of the lack of knowledge regarding the long-term behavior of buildings. High-rise buildings are the most frequently monitored during extreme events, using accelerometers (e.g. [2–4]), inclinometers (e.g. [4, 5]) and/or GPS-based sensors (e.g. [5–7]). These methods provide important information regarding

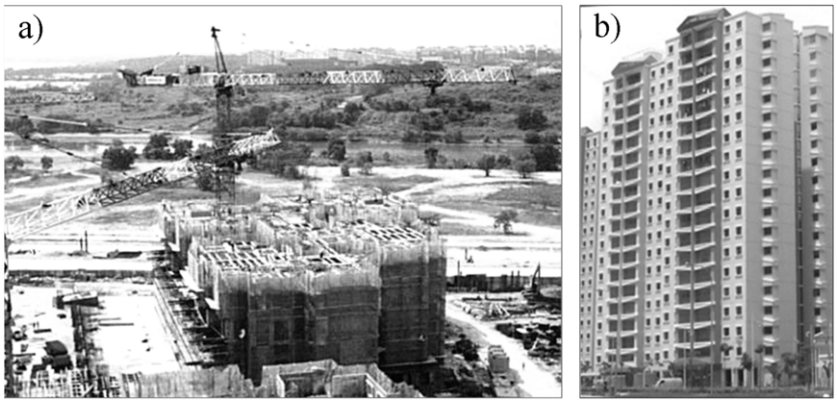

Figure 1. Building at Punggol EC26: (a) during construction and (b) upon completion [8].

the building's behavior during the event and help post-event evaluation. However, a limitation of vibration-based techniques is that they cannot be used to assess slow changes in structural behavior, e.g. due to differential settlements of foundations or rheologic redistribution of the loads. The GPS-based techniques can be used for long-term monitoring, but their performance may be challenged in cases where the slow changes in structural behavior do not generate significant global displacements. This paper presents an alternative approach based on strain monitoring using long-gauge fiber optic sensors. The most important advantages of fiber optic strain sensors are high accuracy and long-term stability, durability, and insensitivity to electro-magnetic influences, corrosion and humidity. References [8, 9] discuss the advantages and implementation of fiber optic sensors in more detail, and present successful examples of their application to SHM of buildings.

The overall objective of this research has been to develop an affordable method for SHM of residential buildings, which can detect slow changes in structural behavior and provide long-term performance. The method includes selection of the monitoring system, design of the sensor network, and development of data analysis algorithms. It focuses on long-term static monitoring based on strain sensing and it can be considered as complementary to the other, above-mentioned methods for SHM of buildings.

The aims of this paper are the following: (1) to present all aspects of an SHM method based on static strain measurements, as applied in a real project (with all the associated limitations imposed by the real-life setting), (2) to demonstrate, through a real example, the value of the presented SHM method, and (3) to provide insight into the real-world long-term structural behavior of high-rise buildings. The method has been applied for more than ten years on a Punggol EC26 high-rise residential building in Singapore, and its successful application and the rich results gathered have led to instrumentation of more than 400 other buildings.

The project realization was subjected to real-life limitations, such as those related to cost constraints and safety issues. As a consequence of the former, a limited number of sensors were installed. As a consequence of the latter, accessibility to sensors at different stages of the project was limited, and thus there is some missing data in the results of monitoring. In addition, some data related to design and structural analysis is not publishable. In spite of these limitations, the project yielded very important insights into real structural behavior that are presented in the paper.

The paper is organized as follows. The instrumented structure and monitoring strategy are presented first, followed by the chosen sensor topology and network. Local and global monitoring results are then presented and analyzed. Finally, results and conclusions are summarized.

2. Punggol East Contract 26, block 166A

The Housing and Development Board (HDB), as Singapore's public housing authority, has an impressive record of providing a high standard of public housing for Singaporeans through a comprehensive building program. As a part of safety and quality assurance of new HDB high-rise buildings, it was decided to perform long-term SHM of new buildings of the development project Punggol East Contract 26 [10]. A view of the building under construction and after completion is presented in figure 1.

This monitoring project was considered as a pilot project with three aims: (1) to develop a monitoring method for column-supported structures such as high-rise buildings, (2) to collect long-term data in order to increase knowledge on its real structural behavior, and (3) to assess the health condition of the building. The monitoring had to include the whole lifespan of the building, from construction to in-use. The Punggol EC26 project consists of six blocks founded on piles, and each block is a nineteen-story tall building, consisting of six units and supported on more than 50 columns at ground level. The block called 166A was selected for monitoring.

3. Monitoring strategy

3.1. Monitoring criteria

Several monitoring criteria have influenced the development of the monitoring method [10]:

(1) Singapore is neither in an important seismic area nor in an area exposed to strong winds (e.g., [11–13]); this combined with a limited budget for monitoring led to the decision not to perform dynamic monitoring.
(2) Critical members had to be monitored, i.e., those in which malfunctioning or failure would generate partial, or even complete, malfunctioning or failure of the structure.
(3) Monitoring had to be performed at both local and at global structural levels; as the knowledge concerning the behavior of one or a few columns is not sufficient to make conclusions concerning the global structural behavior, a representative number of columns had to be equipped with the sensors.
(4) The budget allocated to monitoring activities was limited; in addition, being a pilot project which contained some uncertainties and was subject to development and changes, it was decided to limit the number of sensors installed in the building and to concentrate on the results obtained from this limited number of sensors in order to evaluate the method and improve its performance.
(5) The selected monitoring system had to be designed for structural monitoring, i.e., it had to be free from the influence of local concrete inhomogeneity; consequently the sensors had to have long gauge length [14, 15].
(6) The monitoring was to be performed over the whole lifespan of the structure, including the construction phase; the monitoring system selected for this type of monitoring had to have appropriate performance, notably it had to feature high accuracy and long-term stability; this criteria indicated fiber optic technologies [16] as possible solutions.
(7) For aesthetic reasons it was not permitted for sensors and sensor cables to be visible or to egress directly from the columns; thus the sensors and accessories had to be embeddable in the concrete.

The presented criteria called for a particular monitoring strategy including (1) the selection of the sensor positions, (2) the selection of the monitoring system, (3) the establishment of a measurement schedule, and (4) the development of algorithms for data analysis [10].

3.2. Selection of sensor positions and the monitoring system

Selection of the columns to be instrumented with sensors was constrained by criteria 1–4 above, and was based on building design and structural analysis. Several columns at ground level were identified as critical members (based on structural analysis used in design of the building) and it was decided to instrument ten of them, shown in figure 2, that were estimated to be the most critical.

Selection of the monitoring system was constrained by criteria 1 and 5–7 above. The fiber optic long-gauge strain monitoring system SOFO [17] based on low coherence interferometry was selected, as it fulfils the project requirements, i.e., it features excellent long-term stability, insensitivity to electro-magnetic interferences,

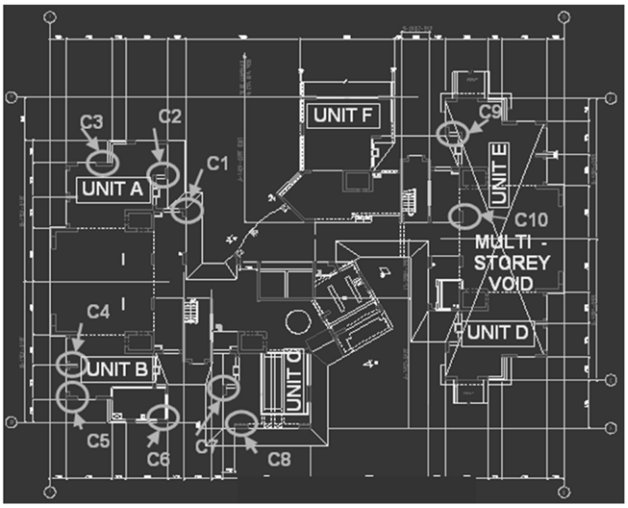

Figure 2. Monitored columns (denoted with C1–C10), ground floor [8].

humidity, and corrosion, physical robustness necessary for safe and easy handling and embedding in concrete [18], and excellent measurement performance—a resolution of 2 μm independent of the gauge length and linearity better than 0.2% of measured deformation [17–19]. Random error of the system was equal to the resolution, while the relative systematic error was equal to the linearity. In addition, the sensors are self-compensated (insensitive) to temperature changes, which is enabled by the use of measurement and reference optical fiber, the former coupled with the structure and the latter strain free (see more details in [8, 17–19]). A more extensive literature review on long-gauge fiber optic sensors is omitted here, as it falls outside the topic of the paper, however the interested reader can find more data in ([14, 16–21], etc).

As the purpose of monitoring was global evaluation of the structural health condition rather than understanding how the stresses redistribute locally in the column, it was decided to use long-gauge sensors. The length of the sensors was determined as a combination of the available height of the column (3.5 m), on-site conditions, and accuracy concerns related to gauge length (see [14]); hence, 2 m long sensors were used. The general advantages of long-gauge sensors are insensitivity to local material inhomogeneities present in concrete [14] and enhancement of damage detection thanks to the long-gauge length (2 m/3.5 m = 57% of the column length is equipped with sensor). The error limits of measurement in terms of average strain were 1 $\mu\varepsilon$ (2 μm/2 m) or 0.2% of measured average strain, whichever is higher.

Based on design and construction details, the dominant load in each column is compressive axial force; therefore, the influence of bending to deformation is minimal. Consequently, a single sensor per column, installed parallel to the column axis, and not necessarily in the center of gravity of the cross-section, was estimated as sufficient for monitoring at the local column level. Some bending in columns certainly occurs due to interaction with horizontal frames, foundation imperfections, and eccentricity of the axial force. The former

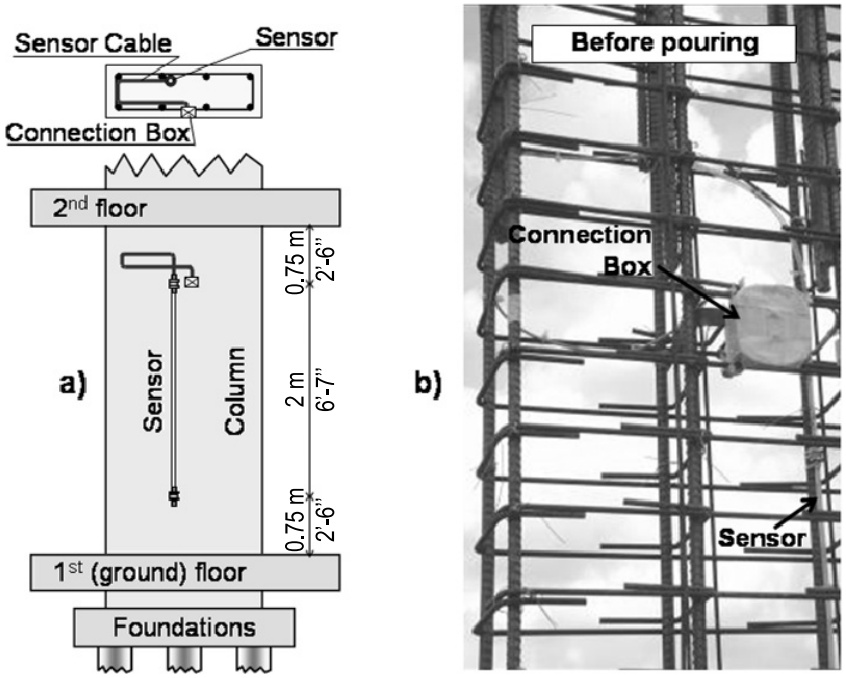

Figure 3. (a) Position of sensor in a column and (b) sensor attached to a rebar before pouring [8].

two create a linear bending moment distribution along the column with extreme values at the top and bottom of the column and an inflection point (zero moment) at approximately half height of the column. The sensor's long gauge further minimizes the effects of this bending moment on the measurement, as the center of the gauge length is close to the inflection point. Bending moments due to eccentricity of axial force, although minimal, affect the measurement, and its influence is accounted as error in measurement of axial strain. The influence of bending moments generated by eccentricity was confirmed to be minimal by a separate study based on Eurocode 2 and Bayesian data analysis (for more details see [22]). The position of sensor in the column is presented in figure 3. The eccentric positions with respect to the columns' centroids were imposed by real-life limitations: as the sensor is soft (to allow easy handling of 2 m long sensors and enhance strain transfer from concrete at early age [18]) it is straightened and simply attached to the rebars using plastic ties; the installation of sensors in the centroids of columns would require the addition of rebars at these locations, which would present an obstacle for vibrators and would require special approval, the redesign of the columns, and an increased cost of installation.

Singapore is located only 137 km (85 miles) north of the Equator, with a tropical rainforest climate and no distinctive seasons, thus yearly temperature and relative humidity (RH) variations are low. The average daily temperature varies between 23 and 34 °C approximately (extremes 19.4 and 35.8 °C), while the average RH is often higher than 90% in the morning and approximately 60% in the mid-afternoon, with a mean value of 84% [23]. The fact that temperature variations are low in Singapore, combined with the requirement to keep the cost of monitoring contained, led to the decision not to monitor the temperature in concrete. The lack of temperature monitoring introduced uncertainty in the estimation of strain components from measurements, but did not affect the accuracy of the monitoring system as the SOFO sensors are self-compensated to temperature (e.g. [17–19]).

3.3. Schedule of measurements

In order to decrease the cost of monitoring, it was decided not to centralize the system and to perform measurements manually during scheduled field measurement sessions. During the construction period, one measurement session was performed upon completion of each new story and the roof. After the construction, the measurement sessions were carried out less regularly, typically few times a year. However, in order to evaluate the influence of combined daily fluctuations of temperature, humidity, and live load, 48 h continuous sessions were performed in years 2004–7, i.e., when these fluctuations became the most dominant deformation factor. In addition, the 48 h continuous sessions are also used as baselines for data analysis and detection of unusual behavior. Finally, special measurement sessions were envisaged upon extreme events, and one such a session was performed after the tremor generated by the earthquake in neighboring Indonesia in 2005.

3.4. General description of data analysis algorithms

The data analysis was performed at the local member level and the global structural level. Local member analysis focused on the strain magnitude measured in each individual column, while global structural analysis focused on the behavior of the building as a whole. Local level analysis consists of

Table 1. Input parameters for estimation of creep based on different codes (adapted from [25]).

	Influencing factor	ACI-209 (USA)	JSCE (Japan)	BP-KX (UK)	CEB/fip MC90	Practical design recommendations (simplified MC90)
Internal	Unit cement	X	X	X		
	Unit water		X			
	W/C		X	X		
	Unit weight	X		X		
	Compressive strength			X	X	X
	S/A			X		
	Slump	X				
	Air content	X				
	Cement type			X	X	
	V/S	X	X	X		
	Notional size	X	X		X	X
External	Curing duration	X				
	Curing method	X		X	X	
	Curing temperature			X	X	
	Relative humidity	X	X	X	X	X
	Age at loading	X	X	X	X	X

three parts: (i) comparison of long-term measurements with a numerical model to detect unusual behaviors and assess the actual performance of the columns, (ii) comparison of the estimated elastic strain with limit states to assess the structural safety of the columns and (iii) comparison of short-term strain changes with the baseline measurements (from 48 h sessions) to identify changes in columns' structural behavior caused by hazardous events. Global level analysis consists of two parts: (i) analysis of linear correlations among the groups of sensors belonging to the same unit to identify local changes in structural behavior (e.g. differential settlement of foundations) and (ii) analysis of linear correlations among all the sensors in the building to identify global changes in structural behavior (e.g. inclination of the building or drifting of the upper floors). Algorithms applied in local (member) analysis are presented first, followed by algorithms for global (structural) analysis.

The long-gauge sensor measures the average total strain over its gauge length [14], and for mature concrete the measured strain under usual conditions consists of four common components: elastic strain, creep, shrinkage, and thermal strain [15, 16]. The sensor measures the sum of these components (total strain), but the estimation of individual components from measurements is very challenging, as it would require determination of creep and shrinkage through long-term tests, which would involve high costs. Thus, comparison with a numerical model was chosen as a more economic option. However, creation of an accurate numerical model that accounts for creep and shrinkage would require the determination of input parameters that can only be obtained from similar expensive tests. That is why the data is analyzed at the local column level by comparison of the results with a numerical model based on the simplified CEB-FIP Model Code 1990 (MC90), i.e. on practical design recommendations [24] based on MC90. This simplified version of MC90 (i.e., practical design recommendations [24]) was chosen due to numerous uncertainties related to concrete properties and ambient conditions. It deals with minimum external parameters and makes the analysis less complex. Any other code-based model needs more parameters, which were not all available due to cost limitations and safety concerns. As an illustration, parameters influencing the creep as per various codes are given in table 1 (adapted from [25]).

The expressions (1) and (2) were used to estimate creep and shrinkage at time t after the pouring [24]:

$$\varepsilon(t) = \sum_{i=1}^{n} \Delta\varepsilon_{E,i} K_{\varphi,i} f_{\varphi,i}(t) \tag{1}$$

where n = number of load increments, ε_φ = creep, $\Delta_{E,i}$ = strain component generated by loading i (elastic strain), $K_{\varphi,i}$ = mean creep coefficient dependent on the notional size (effective size member), relative humidity and age at time of application of loading i, $f_{\varphi,i}(t)$ = creep function ranging between 0 and 1, dependent on the notional size (effective size member) and age at time of application of loading i;

$$\varepsilon_{Sh}(t) = \varepsilon_{Sh,max} f_{Sh}(t) \tag{2}$$

where ε_{Sh} = shrinkage, $\varepsilon_{Sh,max}$ = mean final shrinkage dependent on the notional size (effective size member) and relative humidity, $f_{Sh}(t)$ = shrinkage function ranging between 0 and 1, dependent on the notional size (effective size member).

It was first verified that all the necessary assumptions were satisfied, i.e., the concrete has aged more than 28 days, was built of normal weight aggregate, with grade ranged between 20 and 50 MPa, subjected to compression stress not exceeding $0.4f_{ck}$ (f_{ck} = 40 MPa, characteristic cylinder strength at 28 days). The load level in columns is relatively low, and the stress–strain relation of concrete could be modeled as linear elastic. In order to simplify analysis it was assumed that loads were applied in discrete increments, e.g. one built story is considered as single change in load. One increment of load during the construction corresponds to the

Table 2. Cross-sectional properties of columns.

		Column[a]								
		C1	C2	C3	C4	C5	C6	C8	C9	C10
$A_{concrete}$	($\times 10^3$ mm^2)	300	270	420	405	315	300	360	195	300
A_{steel}	($\times 10^3$ mm^2)	2.011	2.513	8.168	2.815	2.011	2.513	8.836	3.927	8.621
Exposed perimeter[b]	(mm)	2600	2400	3400	3300	2700	2600	3000	1900	2600
Effective member size[b]	(mm)	231	225	247	245	233	230	240	205	230

[a] Geometrical data for column C7 were not available. [b] As defined in [24].

Table 3. Estimated final (long-term) values of strain components and total strain.

	Column[a]								
	C1	C2	C3	C4	C5	C6	C8	C9	C10
Load level (%)	20.4	20.9	32.1	17.0	19.5	19.6	20.9	30.0	32.7
Elastic strain (design) ($\mu\varepsilon$)	−226	−165	−325	−187	−209	−251	−272	−259	−323
Final creep (MC90) ($\mu\varepsilon$)	−284	−208	−401	−230	−262	−315	−339	−320	−380
Final shrinkage (MC90) ($\mu\varepsilon$)	−314	−315	−312	−312	−314	−314	−313	−319	−314
Total estimated strain ($\mu\varepsilon$)	−824	−688	−1038	−729	−784	−879	−924	−898	−1017

[a] Geometrical data for column C7 were not available.

dead-load generated by one new story or the roof. The exact load increments could not be measured and the design values have been used for modeling.

Values of mean final creep coefficients and creep function are calculated using linear interpolation of values given in practical design recommendations [24] based on MC90 (table 2.3 and figure 2.7(b) respectively, both given in [24]). Values of mean final shrinkage and shrinkage function are calculated using linear interpolation of values given in the practical design recommendations [24] based on MC90 (table 2.3 and figure 2.7(b) respectively, both given in [24]). The creep and shrinkage were modeled for each monitored column using the time of concrete pouring as a reference and conservative average RH of 75%. The RH of 75% is chosen as a compromise—the columns are on one face exposed to outdoors (mean RH 84%), and on the other face exposed to indoors (lower RH). The creep was estimated, taking into account the real loading incremental schedule during construction as reported from the contractor, while afterwards the schedule of loading was based on an averaged increase in building occupancy rate.

The columns were built using common concrete mix, with Young modulus of 28 GPa at 28 days. The shapes of columns, cross-sections and their exposure to environment, as well as design dead and live loads are different from column to column. Geometrical properties of cross-sections are presented in figure 2 and table 2.

Since the temperature was not monitored, the thermal strain could not be estimated. Hence, under the normal (usual) structural condition the total strain at time t after the pouring was estimated as a simple sum of elastic strain, creep and shrinkage, while the thermal strain was included in the measurement error. The final values of all considered strain components and the total estimated strain for each column are given in table 3 and graphically represented in figure 4. The load level, calculated as the ratio between the design axial force in the column and product of concrete compressive strength and area of cross-section, is given in the same table.

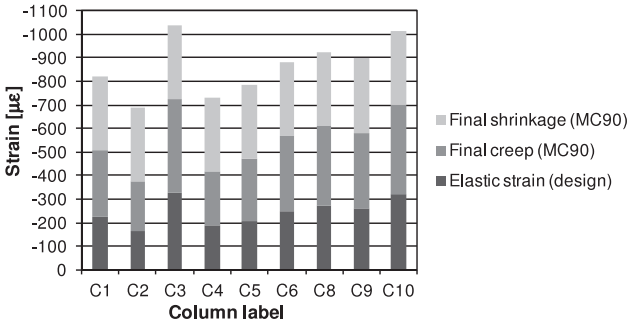

Figure 4. Final strain components as estimated from design and simplified MC90.

Pouring of columns was made on 11 April 2001. The reference measurement was performed after the second story was built, i.e. 43 days after the pouring of columns and 15 days after the pouring of the first story, and the elastic strain generated by the first two stories, creep generated over 15 days by the first story dead-load, and the shrinkage developed over the first 43 days were not included in monitoring. These values are estimated using simplified MC90 [24] and presented in table 4.

The data was analyzed at the global structural (building) level by correlating measurements from different columns. This approach is presented in more detail. Supposing the story slab and horizontal beams are provided with high stiffness, (1) the columns supporting the slab are expected to deform for similar absolute values and (2) the total strains in different columns are expected to be in mutual linear correlation. The two criteria presented above are, in general, used to detect imperfections in column-supported structures as described in [8]. An illustration of the method for detection of unequal foundation settlement is presented in figure 5(a) [8]. The

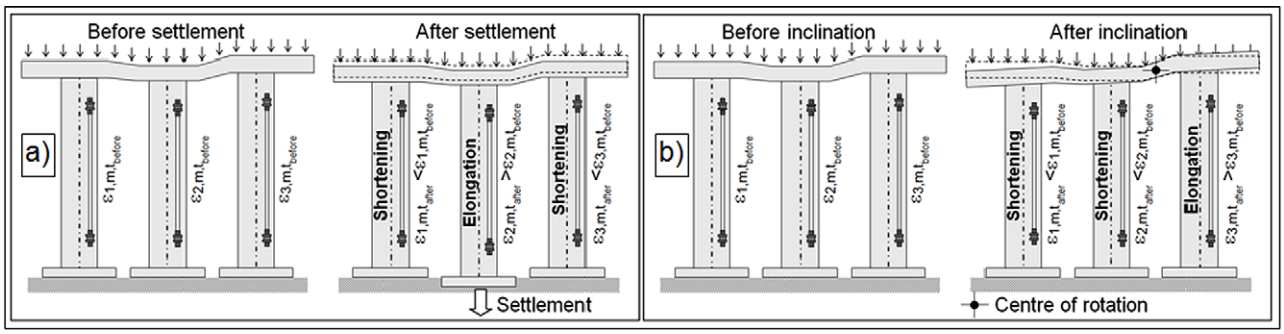

Figure 5. Schematic representation of (a) detection of differential settlement of foundations and (b) detection of inclination of the story [8].

Table 4. Estimated strain components and total strain that were not included in monitoring.

	Column								
	C1	C2	C3	C4	C5	C6	C8	C9	C10
Elastic strain first and second story ($\mu\varepsilon$)	−22	−16	−31	−17	−20	−24	−26	−10	−6
Creep from first story at 15 days ($\mu\varepsilon$)	−4	−3	−5	−3	−3	−4	−4	−2	−1
Shrinkage at 43 days ($\mu\varepsilon$)	−49	−50	−48	−48	−49	−49	−48	−52	−49
Total not included in monitoring ($\mu\varepsilon$)	−75	−69	−83	−68	−73	−78	−79	−64	−56

column with foundation subject to settlement will elongate while the neighboring columns will shorten. In this case the linear correlation between the elastic strains of the columns is lost. Moreover, the strain changes in the column whose foundation is subjected to settlement will become very small, i.e., the strain in the column will become almost constant. Similar to the previous example, an inclination of the building story as a whole is detected from unequal deformation of the columns, as presented in figure 5(b) [8], the deformation of columns found on one side of the center of rotation of the building will systematically decrease while the deformation of the columns found on the other side will increase. Besides the descriptive analysis presented above, statistical analysis and, in particular, analysis of linear correlations between the measurements of different sensors can ascertain the structural malfunction. In particular, linear correlations between the columns will be preserved, but the slopes of these correlations will change (correlations will feature bilinear behavior). A permanent story drift will change the position of the centroid of weight of the building, which in turn will change the global static moment with respect to the centroid of stiffness of the ensemble of columns and affect the redistribution of axial forces (and strains) in columns, with consequences similar to inclination of a building story. Distinction between story drift and inclination can be made by an additional inspection.

Collected data was stored automatically in the SDB relational database [26]. The SDB software suite [27] is used for data analysis and visualization. The 'SDB Pro' plug-in module [28] was upgraded with a novel 'macro-sensor' called 'Concrete Analyzer', which enabled direct comparison between the measurements and estimations based on simplified MC90, i.e., it enabled automatic data analysis at the local level. The analysis at the global level was performed using standard 'macro-sensor' functions of 'SDB Pro'. The 'SDB View' plug-in module [29] was used for data visualization and alarm.

4. Results and analysis

4.1. General

The measurement of a long-gauge sensor embedded in concrete represents the total average strain change with respect to the reference time. It includes the sum of several strain components, which for mature concrete under usual conditions can be represented by expression (3)

$$\Delta\varepsilon_{\mathrm{s}} = \Delta\varepsilon_{\mathrm{E}} + \Delta\varepsilon_{\varphi} + \Delta\varepsilon_{\mathrm{Sh}} + \Delta\varepsilon_{\mathrm{T}} \tag{3}$$

where $\Delta\varepsilon_{\mathrm{s}}$ = change in total strain measured by sensor, $\Delta\varepsilon_{\mathrm{E}}$ = strain component generated by stresses, $\Delta\varepsilon_{\varphi}$ = creep, $\Delta\varepsilon_{\mathrm{Sh}}$ = shrinkage, and $\Delta\varepsilon_{\mathrm{T}}$ = thermal strain (total strain and all strain components represent changes with respect to the reference time).

Since the temperature changes in Singapore are small, the temperature was not measured, and the thermal strain could not be determined. It was assumed that thermal strain can be neglected, i.e., $\Delta\varepsilon_{\mathrm{T}} \approx 0$, and consequently expression (3) simplifies to:

$$\Delta\varepsilon_{\mathrm{s}} \approx \Delta\varepsilon_{\mathrm{E}} + \Delta\varepsilon_{\varphi} + \Delta\varepsilon_{\mathrm{Sh}}. \tag{4}$$

In expression (4), the thermal strain is actually considered as the error in measurement of the sum of the elastic strain, creep and shrinkage. The error introduced by the lack of temperature monitoring was assessed during the four 48 h continuous measurement sessions performed in years 2004–7. Maximal variation of the strain due to daily temperature variations was evaluated and extrapolated to yearly variations. This was possible assuming that during those 48 h the load in the building does not change significantly (only occupants moved in and out on daily business), while the changes in the creep and shrinkage could be neglected for such a short period of time.

Table 5. Estimated error limits in total strain measurement based on assessment of thermal strain variations and the error limits of the monitoring system.

	Column								
	C1	C2	C3	C4	C5	C6	C8	C9	C10
Air temperature variation producing largest strain variation during 48 h sessions (°C)	5.0	5.0	5.0	5.0	3.0	3.0	5.0	5.0	5.0
Daily thermal strain variation estimated from 48 h sessions ($\mu\varepsilon$)	10.0	10.5	8.0	11.5	17.0	23.0	8.5	8.5	10.0
Yearly strain variation estimated by extrapolation for expected temperature variation of 11 °C ($\mu\varepsilon$)	±11	±12	±9	±13	±45	±48	±13	±9	±11
Error limits of the monitoring system for measured strain up to 500 $\mu\varepsilon$ ($\mu\varepsilon$)	±2	±2	±2	±2	±2	±2	±2	±2	±2
Error limits of the monitoring system for measured strain up to 1000 $\mu\varepsilon$ ($\mu\varepsilon$)	±3	±3	±3	±3	±3	±3	±3	±3	±3
Error limits $e(\varepsilon_s)$ of total strain measurement (as considered in expression (4)) ($\mu\varepsilon$)	±14	±15	±12	±16	±48	±51	±16	±12	±14

Thermal strain in columns was influenced by their exposure to both the sun and the air-conditioned areas. Hence, the daily strain variations were different for different columns. In particular, columns C5 and C6 were about three to four times more sensitive to ambient air temperature changes than the other columns. Maximal changes of temperature and strain registered during these 48 h sessions are given table 5. Their extrapolations to maximal average yearly temperature variations are given in the same table. Finally, the maximal estimated error in total strain measurement is given in the same table, taking into account the random error of the monitoring system, which is estimated to br 1 $\mu\varepsilon$ (2 μm over the gauge length of 2 m), and systematic error, which is estimated to be 1 $\mu\varepsilon$/500 $\mu\varepsilon$ of measured strain.

4.2. Results

The results of monitoring are presented in figure 6. The diagrams presented in figure 6 all have similar shapes; nevertheless, three main behavioral groups are identified.

(G1) Group 1 is formed by columns C2, C4, C6, C7, and C10, in which total strain evolution diagrams do not feature observable irregularities.

(G2) Group 2 is formed by columns C1, C5 and C8, in which the absolute total strain increase is the highest and is particularly unusual in periods September 2002–March 2003 and November 2003–January 2004, probably due to transfer of load from neighboring columns caused by rheologic effects, differential settlement, and interaction with horizontal structural members (beams and slabs); for column C1 irregular behavior is also present in the period after September 2009.

(G3) Group 3 is formed by columns C3 and C9, in which behavior appears as unusual: the absolute value of the total strain of column C9 is significantly lower than both estimated and measured values in the other columns, indicating probable transfer of load to neighboring stiff core and/or overestimation of load, while column C3 features an extremely low increase in compression after September 2002 that changes to relaxation (tension) after January 2005—behavior typical for a column whose foundation is subject to differential settlement (see figure 5(a)); the detected unusual behavior is discussed in more detail in the sections on data analysis (sections 4.3–4.6).

Three periods in strain evolution are identified in figure 6:

(P1) Period 1. May 2001–July 2002 is the construction period, and all the factors: load, creep, shrinkage, and temperature variations contribute significantly to total strain.

(P2) Period 2. July 2002–January 2005, in which creep and shrinkage have the dominant influence on total strain.

(P3) Period 3. January 2005–January 2011, rheologic strain components stabilize slowly (creep developed ∼97% and shrinkage ∼84%, estimated using MC90) and the strain fluctuations due to temperature daily variations become more visible (see 48 h sessions in figure 6, and for example, period 22 January–22 September, 2009).

4.3. Analysis at local, member level—long-term results

At the local structural level, the strain in columns was first compared with the model. The monitoring results and the simplified MC90 model are not expected to match perfectly due to several simplifications that involve both monitoring method and the model. The following imperfections influence, in the most significant manner, the difference between the model and measurements (other imperfections are present but their influence is not very significant, see [8, 10] for more details):

(E1) The temperature of columns was not monitored: the temperature variations were small and the 48 h sessions performed each year in period 2004–7 had shown that they did not significantly influence total strain variations in columns, which can be explained by the reduced

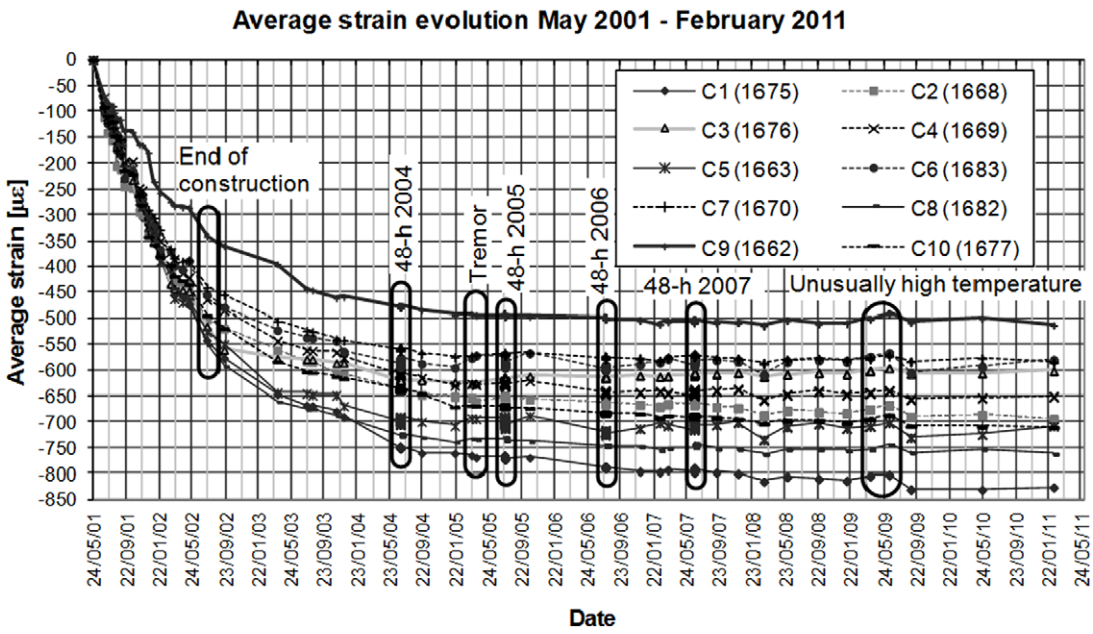

Figure 6. Total strain evolution in columns registered during approximately ten years.

exposure to sun and changed thermal conditions in the completed building; however, in the construction phase the columns were exposed to sun and the thermal strain could significantly influence the value of total strain during that period; in particular, a bias could have been introduced while performing the reference measurement; the influence of temperature variations is estimated in table 5.

(E2) Uncertainties related to loads: the elastic strain was calculated using design values, which are however only the estimates based on expected weight of material, concrete mechanical properties and structural interaction between columns and horizontal members—slabs and beams; rheologic strain components were not taken into account in the design and, consequently, redistribution of loads and elastic strain among the columns due to creep and shrinkage were not included in calculating the elastic strain.

(E3) Uncertainties related to real structural behavior: an unusual structural behavior (e.g. differential settlement of foundation or higher stiffness of horizontal structural members) may cause non-designed redistribution of load among the columns and increase the difference between the model and the measurements; bending in columns was not expected, and its influence on the measurement was expected to be negligible; however, due to real-life construction imperfections it was probably not completely canceled, and thus it contributes to a difference between the model and the measurements.

(E4) Accuracy of modeling based on simplified MC90: the rheologic strain components are estimated using practical design recommendations based on MC90, which proposes simplified algorithms for an average concrete, without taking into account several factors that influence development of creep and shrinkage, such as type of cement, water–cement ratio, real variations of relative humidity and temperature, etc, and in addition simplified linear behavior of concrete is assumed; the simplifications in the model certainly influence the accuracy of estimation of total strain and consequently affect the comparison with measured values.

Hence, it was very difficult to estimate the goodness of the comparison, as the discrepancy between the model and the measurements, besides the error of the monitoring system, largely depends on the error in model. A literature review [30] showed that the coefficient of variation (ratio between standard deviation and the mean) as a measure of discrepancy between the measurements and models based on various codes can vary for creep only between 6% and 83%. Moreover, in the extreme cases the discrepancy between the measured total strain and the models can be as large as several times (e.g., [31]). MC90 gives estimations of a mean coefficient of variation for the predicted creep function of 20%, and for predicted shrinkage function of 35% (ACI estimations are 41% and 30% respectively). An additional source of error is modeling of elastic strain at the location of the sensor, which depends on the Young's modulus of concrete and loads and also on the eccentricity of the axial force in the column and the eccentricity of the sensor with respect to the centroid of the column. Taking into account all the above influences, and based on tolerances for determination of loads, known eccentricity of sensors and an assumed eccentricity of axial force of 15%, the uncertainty in modeling (equivalent to coefficient of variation) of elastic strain at the location of the sensors was estimated to 25%. Since the strain components are not mutually independent (for example, creep and elastic strain both depend on load, while creep and shrinkage both depend on relative humidity), it is very difficult to accurately

estimate the uncertainty of the modeled total strain (which is the sum of the strain components). That is why, based on Cauchy–Schwarz inequality for covariance, expression (5) was used to estimate the uncertainty in modeling the total strain:

$$\delta\left(\varepsilon_{\text{model}}(t)\right) \leq \frac{v_{\text{load}}\varepsilon_{\text{E,model}}(t) + v_{\varphi}\varepsilon_{\varphi,\text{model}}(t) + v_{\text{Sh}}\varepsilon_{\text{Sh,model}}(t)}{\varepsilon_{\text{E,model}}(t) + \varepsilon_{\varphi,\text{model}}(t) + \varepsilon_{\text{Sh,model}}(t)} \quad (5)$$

where δ denotes (relative) uncertainty, and v denotes uncertainty (coefficient of variation) in strain components ($v_{\text{load}} = 0.25$, $v_{\varphi} = 0.30$ and $v_{\text{Sh}} = 0.35$ as per above discussion).

The (relative) uncertainty presented in expression (5) is determined based on statistical analysis using standard deviation as its measure. Expression (5) is actually a non-conservative limit estimation of uncertainty in modeling, because the actual uncertainty is smaller due to dependences among the strain components. The uncertainty of the model depends on the magnitude of the strain and, as the latter depends on time (adding of load, rheological strain), it also depends on time. The uncertainty calculated based on expression (5) for each column at various times ranges between 25% and 27%. This value (around 25%) is in accordance with the authors' personal experience and also with the study presented in [32]. The practical interpretation of this value is that in 68% of cases the relative difference between the real strain and the model is expected to be within this value. However, this value does define the relative error of the system (as in the other 32% of cases the difference is expected to be outside this value). Nevertheless, the uncertainty in the model is combined with the relative error limit of the monitoring system to compute a threshold value indicating that some unusual behavior may be developing in the structure. The relative error limits of the monitoring system are calculated for each column using the error limits from table 5 and expression (6)

$$\delta(\Delta\varepsilon_{\text{ms}}) = e(\varepsilon_{\text{s}})/\Delta\varepsilon_{\text{m}} \quad (6)$$

where $\delta(\Delta\varepsilon_{\text{ms}})$ = relative error limits of the monitoring system, $e(\varepsilon_{\text{s}})$ = error limits of the monitoring system as given in table 5, and $\Delta\varepsilon_{\text{m}}$ = strain change with respect to reference time estimated by the model.

The threshold, i.e., allowable discrepancy between the measurements and the model is then estimated using expression (7)

$$\pm\delta(\Delta\varepsilon_{\text{s}}) = \pm\delta(\Delta\varepsilon_{\text{ms}}) \pm \delta(\varepsilon_{\text{model}}). \quad (7)$$

Standard deviation, as the measure of uncertainty of the model, does not include all possible cases of agreement between the modeled and true strain (it excludes some 32% of cases). Consequently, a difference between measurements and the model that exceeds the threshold does not necessarily indicate that the structural health condition is severely compromised; it rather indicates an unusual behavior that should be further analyzed in more detail.

In order to simplify the presentation, three moments in time are presented in detail and compared in this paper: (1) the end of construction (19 July 2002, 464 days after the pouring), (2) the measurement performed on 25 September 2008 (2724 days after pouring), and the last available measurement at the time of writing of this paper (11 February 2011, 3593 days after the pouring). The comparison is given in table 6. The values presented in the table take into account estimated strain components not included in monitoring, as given in table 4. Thresholds are calculated for each time stamp and presented in table 6. It is considered that an unusual strain is detected when the relative difference between measurement and the model exceeds the threshold. The detected unusual strains are highlighted in the table. In spite of many sources of errors and uncertainties, the comparison between the modeled and the measured values of total strain is rather good (see table 6), and most of the values are found to be within estimated thresholds. Nevertheless, a few values exceeded the thresholds. The initial findings related to these unusual behaviors are briefly presented in this section, while a more extensive discussion is given in the sections discussing global structural analysis (sections 4.5 and 4.6).

At the end of the construction, two unusual strain values were identified, in columns C2 and C9 (see table 6). The excursion of the strain of column C2 out of the limits during the construction is attributed to its low stiffness; the strain is in the long term redistributed to other structural members due to rheologic effects, and then it falls back within acceptable limits. However, the strain in column C9 has a consistently lower value than expected, and the discrepancy between the measurements and the model increases over time. This is probably due to the transfer of load to neighboring stiff core and/or overestimation of load (i.e., over-dimensioning of the column).

Column C3 also showed unusual behavior in the long term, which is attributed to differential settlement of foundations. The hypothesis that column C3 experiences differential settlement of foundations was further studied and confirmed using a Bayesian analysis of data and a concrete model based on Eurocode 2 (see detailed presentation in [22]). For both detected unusual behaviors further analysis is performed in sections 4.5 and 4.6 (global structural analysis).

The detected unusual structural behaviors indicate minor malfunctioning of structural members and do not represent an issue for structural safety since the elastic strain in concrete is significantly below the ultimate values, i.e., between -1350 $\mu\varepsilon$ (estimated linear elastic limit for compressive strain) and $+60$ $\mu\varepsilon$ (estimated ultimate extension strain).

4.4. Analysis at local, member level—post-tremor evaluation

In March 2005 the earthquake in neighboring Indonesia created a tremor in Singapore. In order to evaluate potential degradation in structural performance a single session over all the sensors was performed immediately after the tremor. Results are presented in figure 7. The change in strain before and after the tremor varied in different columns between -7 $\mu\varepsilon$ and $+5$ $\mu\varepsilon$. This variation is considered as usual, and was attributed to temperature and live load variation rather

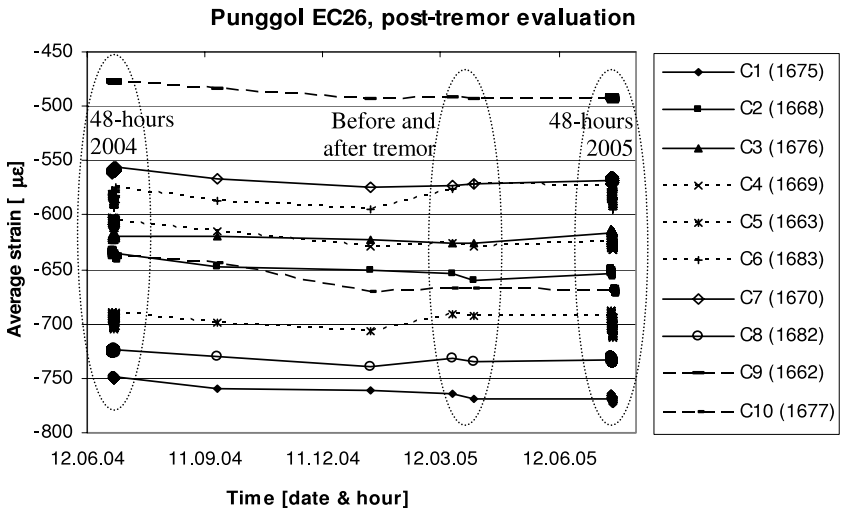

Figure 7. Average strain measurements recorded before and after tremor.

Table 6. Comparison between estimated and measured total strain.

		Column								
		C1	C2	C3	C4	C5	C6	C8	C9	C10
End of construction (464 days after pouring)	Elastic (design) ($\mu\varepsilon$)	−193	−142	−276	−159	−178	−213	−233	−234	−290
	Creep (MC90) ($\mu\varepsilon$)	−185	−137	−254	−145	−170	−204	−219	−201	−223
	Shrink. (MC90) ($\mu\varepsilon$)	−101	−102	−98	−98	−100	−101	−99	−106	−101
	Total (estimated) ($\mu\varepsilon$)	−479	−381	−628	−401	−449	−519	−550	−541	−614
	Total measured ($\mu\varepsilon$)	−576	−519	−560	−485	−549	−479	−592	−359	−519
	Rel. difference (%)	20	**36**	−11	21	22	−8	8	**−34**	−15
	Threshold (%)	±28	±29	±27	±29	±35	±34	±28	±27	±27
After 7 years (2724 days after pouring)	Elastic (design) ($\mu\varepsilon$)	−204	−149	−294	−169	−188	−226	−246	−249	−317
	Creep (MC90) ($\mu\varepsilon$)	−262	−193	−369	−212	−241	−290	−312	−298	−354
	Shrink. (MC90) ($\mu\varepsilon$)	−196	−198	−192	−192	−196	−196	−194	−205	−196
	Total (estimated) ($\mu\varepsilon$)	−663	−540	−855	−573	−626	−713	−752	−753	−868
	Total measured ($\mu\varepsilon$)	−809	−681	−605	−641	−703	−580	−753	−510	−697
	Rel. difference (%)	18	21	**−41**	11	11	−23	0	**−48**	−25
	Threshold (%)	±28	±29	±26	±29	±33	±33	±28	±27	±27
Last available measurement (3593 days after pouring)	Elastic (design) ($\mu\varepsilon$)	−204	−149	−294	−169	−188	−226	−246	−249	−317
	Creep (MC90) ($\mu\varepsilon$)	−274	−202	−386	−222	−253	−304	−327	−309	−367
	Shrink. (MC90) ($\mu\varepsilon$)	−215	−216	−210	−210	−214	−215	−212	−223	−215
	Total (estimated) ($\mu\varepsilon$)	−693	−567	−891	−602	−655	−745	−785	−782	−898
	Total measured ($\mu\varepsilon$)	−826	−694	−601	−650	−707	−580	−762	−513	−710
	Rel. difference (%)	16	18	**−48**	7	7	−29	−3	**−52**	−27
	Threshold (%)	±28	±29	±26	±29	±33	±33	±28	±27	±27

than the tremor, since it was in the range of the previously discussed 48 h variation registered in 2004. As a consequence, the concerns whether the structural safety of the building is compromised or not and should the building be evacuated, were both immediately cleared. Furthermore, the range of 48 h variation of strain registered in 2005, which is similar to that registered in 2004, confirmed that no degradation of performance occurred due to the tremor.

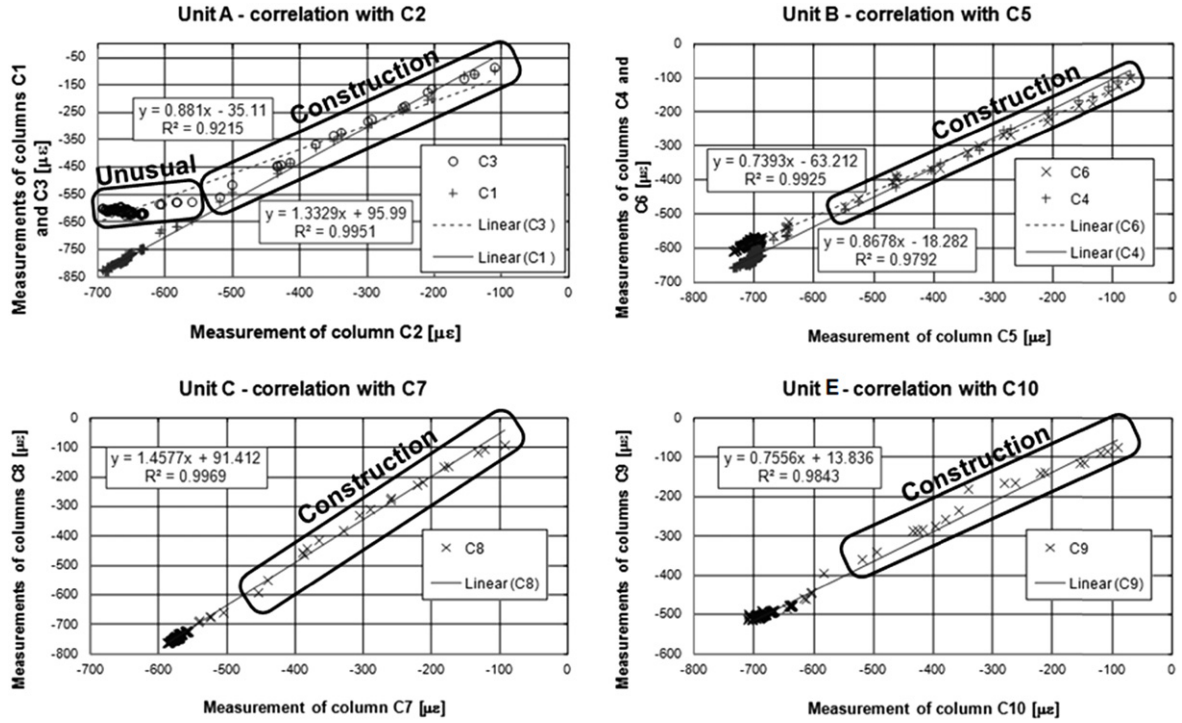

Figure 8. Linear correlations among the strains measured in columns belonging to the same unit.

4.5. Analysis at global, structural, level—construction period

Analysis at the global level is based on a comparison between the strains measured in the columns belonging to the same unit (see figure 2) and globally, between the all instrumented columns. These two types of analyses were performed, both during the construction and in the long term.

Columns C1, C2 and C3 are located in Unit A (see figure 2). During the construction, the average strain measured in these columns is similar in value for each column (see figure 6 and table 6). This indicates that the second floor slab displaced practically as a rigid body. The measured strain and the forces in columns C1 and C2 are slightly higher than values predicted by the model, while in column C3 they are slightly lower. The observed difference is due to redistribution of stresses and strains, which is imposed by the stiffness of the second floor three-dimensional structural frame and interaction with the other columns that have not been equipped with sensors. This statement is loosely supported by the fact that the sum of forces in the concerned columns obtained from monitoring is approximately equal to the corresponding sum obtained from the modeling. The analysis and conclusions concerning Units B and C are the same as for Unit A (see figure 6 and table 6), with the proviso that for Unit C the analysis is less complete and less conclusive since only two columns belonging to this unit have been equipped with the sensors.

Different behavior was noticed in Unit E (see figures 2 and 5). Column C10 has deformed by a similar magnitude as the columns C1 to C8, but the measurement results of column C9 exhibits only approximately 0.63 of the strain in column C10, and this was systematic during the construction (see figure 6). It is important to highlight here that structural conditions of columns C9 and C10 are different from the other columns. In the first six floors of Unit E there are no dwelling units (see multi-story void in figure 2). The space above column C9 is practically empty, while column C10 additionally supports a bridge for connection to building parking. Therefore, the behavior of the three-dimensional structural frame in Unit E is more complex, and its structural analysis was challenging and possible only with limited accuracy. The monitoring has helped in understanding the real behavior of this complex part of the building and indicated the direction for improvement of the design and structural analysis models, and for updating the numerical model of the strain. A similar magnitude in strain, measured in nine out of ten columns, indicated no global rotation or drift of the building floor (see figures 4(b) and 5). Linear correlation between all the sensors during the construction indicated sound structural behavior (see figure 8 in section 4.6). Thus, the unusual behaviors detected during construction in columns C2 and C9 (see section 4.4) were attributed to imperfections in design models (structural analysis) and had no significant influence on the structural health condition of building.

4.6. Analysis at global, structural, level—long-term results

After the construction, the dominant sources of strain are initially creep and shrinkage. After their stabilization the temperature variations became dominant (see figure 6). Creep and shrinkage can generate redistribution of forces among the columns and the redistribution depends on the stiffness of the horizontal structural members (three-dimensional frames and floor slabs). Since the shrinkage is similar for all

columns, and the creep is proportional to elastic strain, the expected redistribution of stresses and strains will reflect small changes in linear correlation between the columns. The linear correlations among the columns belonging to the same unit are shown in figure 8.

The linearity is well preserved in the long term among the strains measured in Units B, C, and E. Linearity in Units B and C confirms that these two units do not experience unusual behaviors. Linearity in Unit E indicates that the behaviors of columns C9 (with smaller detected strain, see section 4.3 on local analysis) and C10 are strongly correlated, which is expected for structures in the linear regime. This is in accordance with the conclusion from local analysis that the design model for column C9 has to be improved and the numerical model for strain evolution updated.

The strain of column C3 features a visible loss of linearity (qualitative change in slope of correlation line, and decrease in linear correlation coefficient, see figure 8). This confirms the unusual behavior of column C3 which was detected in previous, local member analysis. Three of the most likely reasons for unusual behavior are rotation of the floor slab, drift of the floor, and differential settlement of foundations (see figure 5). The measurements did not show inclination or drift of the second-story slab at the building level, as per figure 5(b). Since all the units in the building are interconnected with structural elements it is not likely to expect independent rotation or drift of the second-story slab only in Unit A, unless it is damaged. Visual inspection did not confirm any damage, therefore the most probable reason for discrepancy in column behavior is differential settlement of the foundations. The decrease in absolute strain of column C3 (see figure 6) confirms the hypothesis of differential settlement: column C3 settles and unloads, while columns C1 and C2 take the load and deform more (see figure 5(a)). The preserved linear correlation between columns C1 and C2 confirms that both columns are engaged. The hypothesis that column C3 experiences differential settlement of foundations was further studied and confirmed using a Bayesian analysis of data and a concrete model based on Eurocode (see [22]).

A simplified structural analysis was performed in order to assess the magnitude of differential settlement, showing that the differential displacement among the column tops are in the range of a few millimeters. This small detected anomaly does not present a risk to the structural health of the building. However, monitoring of the strain evolution should continue in order to ascertain whether the differential settlement has stabilized or not, and, in the case of latter, whether there is a necessity for potential rehabilitation of the foundation or not. Detection of this minor unusual behavior demonstrates the sensitivity of the monitoring system and efficiency of the employed monitoring method.

5. Conclusions

A pioneering project on SHM of residential buildings in Singapore is presented. The monitoring method as well as the results collected during approximately ten years are presented and analyzed. The registered parameter was average static strain in columns and it allowed the monitoring of structural behavior at a local (column) and a global (building) level. The project realization was subjected to real-life limitations, such as those related to cost constraints and safety issues. As the consequence of the former, a limited number of sensors were installed. As the consequence of the latter, accessibility to sensors at different stages of the project was limited, and thus some data is missing in the results of monitoring. In addition, some data related to design and structural analysis is not publishable. In spite of these limitations, the project yielded very important insights on the real structural behavior and monitoring method.

Three different periods with various dominant strain components were observed: during the first 1.25 years, approximately all the strain sources (load, rheologic effects, and temperature variations) contributed to total strain; during the next 2.5 years, approximately the creep and the shrinkage dominated; while afterwards the strain generated by temperature variations became dominant (this is, particular for Singapore where there are practically no seasons and temperature variations range between 23 and 34 °C).

The monitored strain in each column was compared with a numerically modeled strain evolution based on the design for an elastic strain component, and simplified MC90 for rheologic strain components. In spite of the limitations imposed by the real-life setting, the comparison demonstrated rather good agreement between the measurements and the model; the relative difference was approximately within ±25% range.

Three behavioral groups of columns were identified—Group 1, with no observable irregularities in behavior, Group 2, with observable irregularities, and Group 3, with unusual structural behaviors. Irregularities in behavior and unusual behaviors are attributed to non-designed redistribution of strain among columns caused by rheologic effects, structural interactions with horizontal members (slabs and beams), and differential settlement of foundations. In particular over-dimensioning of column C9 and differential settlement of foundation of column C3 were detected. The tremor did not affect the structural behavior of columns and the strain change measured after the tremor was within the range measured during 48 h sessions before (2004) and after (2005) the tremor. Consequently, safety concerns were cleared in quasi-real time, and there was no need to evacuate the buildings.

The use of fiber optic sensors on such a large scale for monitoring of high-rise buildings is the first in Singapore and the world, and it sets a direction that will help to better understand the behavior of tall buildings during their life cycle, from construction to service conditions. The employed monitoring system performed very well and all the sensors still functioned properly more than ten years after embedding in concrete. The monitoring method allowed for detection, localization, and quantification of unusual structural behaviors at an early stage and in real-life conditions, confirming its very good performance and demonstrating the high sensitivity of sensors.

The developed monitoring method achieved the objectives of the Punggol EC26 project, and several general

recommendations for SHM of high-rise buildings resulted from the project. In geographic areas with significant daily and/or seasonal temperature variations, it is highly recommended to monitor temperature along with the strain, for an accurate data interpretation and analysis. High-rise buildings are large structures supported by an important number of columns, and this research shows that structural behavior and health condition of the building can be assessed with good accuracy even if a limited number of columns is monitored; however, the total number of the sensors should not be underestimated, and it should be determined based on structural analysis. Simplified modeling of concrete rheologic behavior provided a satisfactory accuracy in data analysis; however, for more accurate data analysis, more sophisticated models may be considered necessary, and their development should happen at an early stage of the SHM project. Depending on the structural complexity of the building more sensors may be needed for a more robust SHM; e.g., several sensors per column are required if bending is expected in the design of the columns, the sensor gauge lengths should be tailored to the expected strain distributions in the columns, and they may be required not only in ground-level columns, but also in higher levels and in some other structural members. More regular (quasi-continues) collection of data could provide a better understanding of daily and seasonal strain variations in the building, allow for more accurate data analysis, and serve for quasi-real-time damage detection. In geographic areas exposed to natural or man-made hazards, particularly to earthquakes and strong winds, dynamic sensors may be needed to assess the structural behaviors during the adverse events. The presented method does not aspire to be the unique method to be applied in high-rise building monitoring or to replace the existing methods; it should rather be observed in the context of information it provides and combined with other methods (e.g. vibration-based methods discussed in section 1) and other sensor configurations (e.g. installed in upper floors or in horizontal structural members) depending on project requirements and on-site setting.

Acknowledgments

The authors would like to thank Mr K P Kwan and the personnel of Sofotec, Singapore, for their valuable help and kind collaboration during the installation of the sensors and for carrying out the measurements. Thanks to Dr Daniele Posenato of SMARTEC, Switzerland, for implementation of the numerical model in the SDB software suite and continuous support on issues related to information technology.

References

[1] NTSB 2011 Pacific Gas and Electric Company Natural Gas Transmission Pipeline Rupture and Fire San Bruno, California, September 9, 2010 *Accident Report* Notation 8275C Adopted 30 August 2011 National Transportation Safety Board (NTSB), www.ntsb.gov/investigations/2010/sanbruno_ca.html (accessed on 3 October 2011)

[2] Mita A, Sato H and Kameda H 2010 Platform for structural health monitoring of buildings utilizing smart sensors and advanced diagnosis tools *Struct. Control Health Monit.* **17** 795–807

[3] Hayashi Y, Sugino M, Yamada M, Takiyama N, Onishi Y and Akazawa T 2012 Consecutive vibration characteristics monitoring of high-rise steel building *Proc. 7th Int. Conf. on Behavior of Steel Structures in Seismic Area, Stessa 2012 (Santiago)* pp 1065–70

[4] Li X, Rizos C, Tamura Y, Ge L, Yoshida A and Cranenbroeck J 2010 Fundamental bending mode and vibration monitoring with inclinometer and accelerometer on high-rise buildings subject to wind loads *5th World Conf. on Structural Control and Monitoring* pp 1–15 Paper No. 160

[5] Cranenbroeck J, Lui V, Li J X and Rizos C 2008 Point attitude determination using inclinometer and GPS for high rise building monitoring projects *Measuring the Changes Proc. 13th FIG Symp. and 4th IAG Symp.* Lisbon Portugal on Conference CD

[6] Hristopulos D T, Mertikas S P, Arhontakis I and Brownjohn J M W 2007 Using GPS for monitoring tall-building response to wind loading: filtering of abrupt changes and low-frequency noise variography and spectral analysis of displacements *GPS Solut.* **11** 85–95

[7] Park H S, Shon H G, Kim I S and Park J H 2008 Application of GPS to monitoring of wind-induced responses of high-rise buildings *Struct. Des. Tall Spec. Build.* **17** 117–32

[8] Glisic B and Inaudi D 2007 *Fibre Optic Methods for Structural Health Monitoring* (Chichester: Wiley) p 262

[9] Moyo P, Brownjohn J M W, Suresh R and Tjin S C 2005 Development of fiber Bragg grating sensors for monitoring civil infrastructure *Eng. Struct.* **27** 1828–34

[10] Glisic B, Inaudi D, Hoong K C and Lau J M 2003 Monitoring of building columns during construction *APSEC: 5th Asia Pacific Structural Eng. & Construction Conf. (Johor Bahru)* pp 593–606

[11] Balendra T and Li Z 2008 Seismic hazard of Singapore and Malaysia *Electron. J. Struct. Eng.* **8** 57–63 Special Issue (Earthquake engineering in the low and moderate seismic regions of Southeast Asia and Australia)

[12] Petersen M, Harmsen S, Mueller C, Haller K, Dewey J, Luco N, Crone A, Lidke D and Rukstales K 2007 Documentation for the southeast Asia seismic hazard maps *Administrative Report of September 30* (Virginia: US Geological Survey Reston)

[13] Kim H G, Lee J H, Jeon W H and Yoon S W 2011 Wind mapping of Singapore by computational fluid dynamics *Proc. Air Quality Modeling in Asia 2011 (Seoul)*

[14] Glisic B 2011 Influence of the gauge length on the accuracy of long-gauge sensors employed in monitoring of prismatic beams *Meas. Sci. Technol.* **22** 035206

[15] Hornby I W 1992 The vibrating wire strain gage *Strain Gauge Technology* ed A L Window (London: Elsevier Science) pp 325–46

[16] Measures R 2001 *Structural Monitoring with Fiber Optic Technology* (London: Academic) p 717

[17] Inaudi D 1997 Fiber optic sensor network for the monitoring of civil structures *PhD Thesis no. 1612,* EPFL Lausanne, Switzerland

[18] Glisic B 2000 Fiber optic sensors and behavior in concrete at early age *PhD Thesis no. 2186,* EPFL Lausanne, Switzerland

[19] Glisic B, Inaudi D, Kronenberg P, Lloret S and Vurpillot S 1999 Special sensors for deformation measurements of different construction materials and structures *Proc. SPIE—Int. Soc. Opt. Eng.* **3670** 505–13

[20] Li S and Wu Z 2007 Development of distributed long-gage fiber optic sensing system for structural health monitoring *Struct. Health Monit.* **6** 133–43

[21] Calderón P A and Glisic B 2012 Influence of mechanical and geometrical properties of embedded long-gauge strain sensors on the accuracy of strain measurement *Meas. Sci. Technol.* **23** 065604

[22] Pozzi M, Glisic B, Zonta D, Inaudi D, Lau J M and Fong C C 2011 Analysis of lifespan monitoring data using Bayesian logic *J. Phys.: Conf. Ser.* **305** 012115

[23] NEA Meteorological Services 2007 *Guide to Singapore's Weather* (Singapore: National Environment Agency) http://app.nea.gov.sg/data/mss/pdf/26March07.pdf (accessed on 15 February 2012)

[24] Fib Commission on Practical Design 1999 *Practical Design of Structural Concrete* (London: SETO)

[25] Song H W, Song Y C, Byun K J and Kim S H 2001 Modification of creep-prediction equation of concrete utilizing short-term creep tests *Transactions SMiRT* vol 16, Paper #1151 (Washington, DC)

[26] Inaudi D, Glisic B and Vurpillot S 2002 Standardization of database structures for monitoring data *IABMAS'02: 1st Int. Conf. on Bridge Maintenance, Safety and Management (Barcelona)* pp 491–2

[27] SMARTEC 2009 *SDB Software Datasheet* No 20.1010, v.2009/09

[28] SMARTEC 2009 *SDB Pro Software Datasheet* No 20.1030, v.2009/02

[29] SMARTEC 2009 *SDB Software Datasheet* No 20.1020, v.2009/02

[30] Bazant Z P, Yu Q, Hubler M, Kristek V and Bittnar Z 2011 Wake-up call for creep, myth about size effect and black holes in safety: what to improve in FIB model code draft *fib Symp. 2011* pp 731–46

[31] Usibe B E, Etim I P and Ushie J O 2012 Prediction of creep deformation in concrete using some design code models *Lat. Am. J. Phys. Educ.* **6** 375–9

[32] Moragaspitiya H N P 2011 Interactive axial shortening of columns and walls in high rise buildings *PhD Thesis* Faculty of Built Environment and Engineering, Queensland University of Technology, Australia, p 157